ORIGINAL RESEARCH

Rhinovirus-induced CCL17 and CCL22 in Asthma Exacerbations and Differential Regulation by STAT6

Teresa C. Williams[1]*, David J. Jackson[2,3]*, Steven Maltby[1], Ross P. Walton[4], Yee-Mann Ching[4], Nicholas Glanville[4], Aran Singanayagam[4], Jennifer J. Brewins[4], Deborah Clarke[4,5], Aurica G. Hirsman[4], Su-Ling Loo[1], Lan Wei[1], Janine E. Beale[4], Paolo Casolari[6], Gaetano Caramori[6,7], Alberto Papi[6], Maria Belvisi[4,5], Peter A. B. Wark[8], Sebastian L. Johnston[4]*, Michael R. Edwards[4]* and Nathan W. Bartlett[1,4]*

[1]School of Biomedical Science and Pharmacy, Faculty Health and Medicine and Priority Research Centre for Healthy Lungs, Hunter Medical Research Institute, University of Newcastle, New Lambton Heights, New South Wales, Australia; [2]Asthma UK Centre, Faculty of Life Sciences and Medicine, King's College London, London, United Kingdom; [3]Guy's Severe Asthma Centre, Guy's & St. Thomas' National Health Service Trust, London, United Kingdom; [4]National Heart and Lung Institute, Imperial College London, London, United Kingdom; [5]Respiratory, Inflammation and Autoimmunity Department, MedImmune, Cambridge, United Kingdom; [6]Interdepartmental Study Center for Inflammatory and Smoke-Related Airway Diseases, Cardiorespiratory and Internal Medicine Section, University of Ferrara, Ferrara, Italy; [7]Dipartimento di Scienze Biomediche, Pneumologia, Odontoiatriche e delle Immagini Morfologiche e Funzionali, Università degli Studi di Messina, Messina, Italy; and [8]Department of Respiratory and Sleep Medicine, John Hunter Hospital, New Lambton Heights, New South Wales, Australia

ORCID IDs: 0000-0002-9807-327X (G.C.); 0000-0001-5676-6126 (P.A.B.W.); 0000-0002-2715-5163 (N.W.B.).

Abstract

The interplay of type-2 inflammation and antiviral immunity underpins asthma exacerbation pathogenesis. Virus infection induces type-2 inflammation–promoting chemokines CCL17 and CCL22 in asthma; however, mechanisms regulating induction are poorly understood. By using a human rhinovirus (RV) challenge model in human airway epithelial cells *in vitro* and mice *in vivo,* we assessed mechanisms regulating CCL17 and CCL22 expression. Subjects with mild to moderate asthma and healthy volunteers were experimentally infected with RV and airway CCL17 and CCL22 protein quantified. *In vitro* airway epithelial cell- and mouse-RV infection models were then used to define STAT6- and NF-κB–mediated regulation of CCL17 and CCL22 expression. Following RV infection, CCL17 and CCL22 expression was higher in asthma, which differentially correlated with clinical and immunological parameters. Air–liquid interface–differentiated primary epithelial cells from

donors with asthma also expressed higher levels of RV-induced CCL22. RV infection boosted type-2 cytokine–induced STAT6 activation. In epithelial cells, type-2 cytokines and STAT6 activation had differential effects on chemokine expression, increasing CCL17 and suppressing CCL22, whereas NF-κB promoted expression of both chemokines. In mice, RV infection activated pulmonary STAT6, which was required for CCL17 but not CCL22 expression. STAT6-knockout mice infected with RV expressed increased levels of NF-κB–regulated chemokines, which was associated with rapid viral clearance. Therefore, RV-induced upregulation of CCL17 and CCL22 was mediated by NF-κB activation, whereas expression was differentially regulated by STAT6. Together, these findings suggest that therapeutic targeting of type-2 STAT6 activation alone will not block all inflammatory pathways during RV infection in asthma.

Keywords: rhinovirus; asthma; STAT6

Rhinoviruses (RVs) are the most frequent virus infections associated with asthma exacerbations (1). Preventing or treating RV-induced asthma exacerbations remains a challenge, as there are currently no effective treatments for RV infection. An improved understanding of the immune response to RV infection is necessary to aid development of new therapies.

The role of type-2 immune responses in the pathogenesis of asthma is well documented (2), and RV infection augments type-2 inflammation (3–5). For example, in experimental RV infections of subjects with atopic asthma, exacerbation severity correlated with T-helper cell type 2 (Th2) cell cytokine production and viral load (3). In type-2 inflammatory airway diseases (e.g., allergic asthma), recruitment of CCR4-expressing immune cells to the airways is regulated by production of chemokines, including CCL17 (6) and CCL22 (7). The relevance of these CCR4 ligands to disease is supported by their increased levels in serum and sputum from patients with asthma (8).

CCR4 is expressed by type-2 inflammatory cells (including Th2 cells (9) and innate lymphoid cells (10)), which produce IL-4, IL-5, and IL-13 and underpin the pathogenesis of allergic asthma (11). Genetic ablation of either CCR4 ligand (CCL17 or CCL22) reduced lung inflammation, decreased Th2 infiltration, and reduced airway hyperreactivity in mouse models of allergic airway disease (6, 12). Monoclonal antibodies targeting CCR4 (e.g., mogamulizumab) have been approved in Japan for the treatment of adult T-cell leukemia–lymphoma (13). Although phase I trials have also assessed CCR4-targeting monoclonal treatment in asthma, those trials were discontinued and have not been further pursued for asthma or viral-induced exacerbations.

Promoter analyses of CCL17 and CCL22 have identified binding sites for NF-κB and STAT transcription factors, consistent with regulation by multiple inflammatory pathways (14–16). Costimulation of human lung epithelial cells with the STAT6-activating cytokine IL-4, and with TNF-α (which activates NF-κB), synergistically induced CCL17 production (17). This highlighted the potential for RV infection–induced NF-κB activation (18) to augment CCL17 in asthma, modulating airway inflammation and disease exacerbation.

There has been long-standing interest in CCL17 and CCL22 as treatment targets for type-2 inflammatory diseases, including asthma. Despite this, there is a limited understanding of whether pulmonary CCL17 and CCL22 production is regulated by STAT6 and/or NF-κB in the context of RV infection and asthma. Furthermore, there is evidence to suggest that the regulation of CCL17 and CCL22 by STAT6 is context dependent (19). We previously reported that RV infection augments CCL17 and CCL22 expression in a mouse model of allergic airway disease (18) and recently reported that both chemokines are induced by RV infection in humans and further increased following infection in people with asthma (20).

In the current study, we investigate relationships between human CCL17 and CCL22 protein expression in the context of allergic inflammation *in vivo* following experimental RV infection of healthy volunteers and patients with atopic asthma. We also used mouse RV infection models to assess functional roles of STAT6 and NF-κB using transgenic and pharmacological interventions. As airway epithelial cells are the primary site of RV infection, we also used *in vitro* human airway epithelial cell RV infection models to assess transcriptional regulation of CCL17 and CCL22. This is the first study to identify correlations between CCL17 and CCL22 airway protein expression and disease parameters associated with RV infection in asthma. We also define the role of key transcription factors (NF-κB and STAT6) in RV and type-2 cytokine induction of these chemokines *in vivo* and by human airway epithelial cells *in vitro*.

Methods

Human Participants

We studied nonsmoking subjects with mild to moderately severe asthma and healthy volunteers aged 18–55 years (confirmed serum RV-A16–neutralizing antibody negative), as previously reported (5). The study received Research Ethics Committee approval (09/H0712/59) and subjects provided informed consent (5). Inclusion/exclusion criteria for subjects with asthma included doctor diagnosis of asthma, airway hyperresponsiveness, evidence of atopy (by skin prick test), and a history of infection-induced asthma

exacerbation (5). Subjects with a history of severe asthma, >5 pack-year history or recent smoking, or current symptoms of allergic rhinitis or who experienced an asthma exacerbation or respiratory virus illness within the previous 6 weeks were excluded. Nonsmoking, nonasthmatic healthy controls were recruited based on no history of asthma, atopy, or allergic disease and no objective airway hyperresponsiveness. For patient demographics and additional information, *see* reference (5).

Human Rhinovirus Challenge

Participants underwent bronchoscopy ∼14 days before inoculation with RV-A16 (21) and on Day 4 after infection. On Day 0, RV-A16 was delivered to both nostrils (100 median tissue culture infectious dose [$TCID_{50}$]) using an atomizer, as previously described (5). Protein mediators in nasal secretions were assessed by nasosorption (Days 0, 2–5, and 7) (5). On Day 4 after infection, bronchosorption was conducted as previously described (20). Diary cards of upper and lower respiratory tract symptoms were commenced before baseline sampling and continued for 6 weeks after RV-A16 infection, as previously described (3, 5). CCL17 and CCL22 proteins in nasal and bronchial secretions were quantified by Meso Scale Discovery multispot human cytokine assay, as described previously (20).

Mouse Rhinovirus Infection

Female BALB/c mice, 6–8 weeks, were purchased from Harlan UK. $Tnfrsf1a^{-/-}$-$Rela(p65)^{+/-}$ mice (129/Sv - C57BL/6 background) were bred to generate TNFR1-deficient mice of $p65^{+/+}$ (wild-type [WT]) or $p65^{+/-}$ (heterozygous) (22). Genotype was determined by PCR. As TNFR1/p65-deficient mice are susceptible to bacterial infections, antibiotics were included in drinking water (23). STAT6 knockout (ko) mice ($Stat6^{tm1/Gru}$–Balb/c background) were purchased from Jackson Laboratory.

RV-A1 (American Tissue Culture Collection) was purified and titrated, as described previously (24). Where indicated, ultraviolet (UV)-inactivated RV-A1 (1,200 mJ/cm^2; 30 min) was used. Mice were infected by intranasal instillation RV-A1 (5×10^6 $TCID_{50}$), as previously described (24, 25). Infectious RV titer in homogenized lung tissue was determined in HeLa H1 cells via TCID50 assay as previously described (24). To inhibit IKK-β in mice, PS-1145 (40 mg/kg in 10% DMSO) was

administered by intraperitoneal injection (Millennium Pharmaceuticals [26]).

At indicated times after infection, BAL was performed and CCL17, CCL22, IFN-λ2/3, CXCL1, and CXCL2 protein levels quantified by ELISA, according to manufacturer instructions (R&D Systems). CCL17 and CCL22 expression in airway epithelium was determined by immunohistochemistry staining of tissue samples.

STAT6 Protein Quantification in Mouse Lung

Lung tissue cell cytoplasmic and nuclear protein extracts were prepared using a CelLytic NuCLEAR extraction kit (Sigma), according to the manufacturer's instructions. Cytoplasmic fraction proteins were resolved by denaturing SDS-PAGE and immunoblotted using antibodies against STAT6-phosphor Y641 (Abcam). electrophoretic mobility shift assay was performed, as previously described (27). Lung tissue nuclear protein extracts were incubated with labeled STAT6-binding DNA probe and binding specificity demonstrated using $100 \times$ excess (20 pmoL) unlabeled DNA. DNA–protein complexes were resolved on native acrylamide gel and visualized by autoradiography.

CCL22 and CCL17 Protein Immunostaining in Mouse Lung Tissue

Single immunohistochemical staining was performed as previously described (28), using goat anti-mouse CCL22 (sc-12288; Santa Cruz Biotechnology) and goat anti-mouse CCL17, respectively (AF529; R&D Systems). Staining was scored by a single, blinded investigator (P.C.) using microscopy. CCL22 and CCL17 epithelial staining was scored as follows: 0 = no staining; 1–4 based on 1–24%, 25–49%, 50–74%, or 75–100% (28, 29).

Human Cell Culture

A549 lung epithelial cells (European collection of authenticated cell culture [ECACC]) were cultured in Dulbecco's modified Eagle medium containing L-glutamine, HEPES, sodium bicarbonate, and 10% FCS. Cells were pretreated with IL-4 (10 ng/ml) 16 hours before infection with RV-A1 (multiplicity of infection [MOI] = 20). Knockdown of NF-κB p65, IKK-β, and STAT6 was achieved using ON-TARGET plus SMART pool siRNA (4 siRNAs per target; Dharmacon/ThermoFisher) and Lipofectamine 2,000 transfection reagent (Invitrogen), as previously described (30). Reduction of targeted protein expression was confirmed by Western blot (30).

BEAS-2B airway epithelial cells (ECACC) were cultured in RPMI 1640 medium with 10% FCS. Transient transfection of BEAS-2B cells with a STAT6-responsive-luciferase reporter plasmid c/EBP-N4-luc (19, 31) was performed, as described previously (18). Briefly, cells were transfected with c/EBP-N4-luc and pRL Renilla luciferase control reporter vector (Promega) in Superfect (Qiagen) transfection reagent, based on manufacturer recommendations. At 24 hours after transfection, cells were treated with IL-4 (10 ng/ml) and/or infected with RV-A1 (MOI = 1). At 24 hours after treatment/infection, luciferase activity in cell lysates were measured using a dual luciferase protocol (Promega).

Bronchial epithelial cells (BECs) from healthy donors and donors with asthma were cultured at air–liquid interface (ALI), as previously described (32). Briefly, BECs were cultured on placental collagen-coated flasks until confluent, then seeded onto transwell inserts at passage 2 in 1:1 mix of Dulbecco's modified Eagle medium and BEBM plus supplements (Lonza). Apical media was removed once cells were confluent and cultures differentiated for 24 days, where evidence of mucus and cilia was present. At Day 24 after ALI, basal media was replaced with minimal BEBM media supplemented with human recombinant IL-4 and IL-13 (10 ng/ml; Peprotech). On Day 25, cells were infected with RV-A1 (MOI 0.1) (33) and harvested 4 days after infection.

Human CCL22 and CCL17 protein in epithelial cell cultures was quantified using DuoSet ELISAs, according to manufacturer instructions (R&D Systems). For STAT6, JAK1, and JAK2 protein expression and phosphorylation analysis, BEC protein lysates were diluted with Laemmli loading buffer, denatured, and run on a TGX 4–12% stain-free gel (Biorad). Membranes were subsequently transferred onto nitrocellulose, blocked in BSA/skimmed milk, and stained overnight for phosphorylated STAT6 (pSTAT6; CST), STAT6 (Santa Cruz), JAK1 (CST), JAK2 (CST), or B-actin (Abcam). Blots were then washed in TBS-T and stained with anti-rabbit and anti-mouse secondary antibodies (Abcam), imaged using a Chemidoc imager (BioRad).

Quantitative PCR

CCL17, CCL22, SOCS1, and SOCS3 mRNA levels were measured by quantitative PCR, normalized to 18S reference gene levels (primer sequences in Table 1). RNA was extracted using an miRNeasy mini kit (Qiagen) and quantified using a nanodrop spectrophotometer. cDNA was generated using Taqman reverse transcription reagents and quantitative PCR performed on an ABI7500 with Quantstudio software (Applied Biosystems).

Statistical Analysis

Statistical analysis was performed using GraphPad Prism v8.2.1 software. A Wilcoxon matched pairs test was used to assess the effect of treatment within a group, and a Mann-Whitney test was used to compare between different groups. For comparisons between multiple groups of nonnormally distributed data, a Friedman test with Dunn's multiple comparison was

Table 1. Clinical Characteristics of Time-Course Donors

	Asthma
Number	6
Age, yr, mean (SD)	58.3 (15.3)
Sex, M/F	1/5
Atopy (SPT positive)	1/6
Severity	
Mild to moderate	5
Severe	1
FEV$_1$, % predicted (SD)	82.5 (11.9)
FVC, % predicted (SD)	89 (8.3)
Daily ICS dose, beclomethasone equivalent, μg (SD)	218.3 (37.6)

Definition of abbreviations: FEV$_1$ = forced expiratory volume in 1 second; FVC = forced vital capacity; ICS = inhaled corticosteroid; SPT = skin prick test.

used. Log-transformed viral load data were compared by two-way ANOVA with Sidak's multiple comparisons test. Transformed data were fitted to a straight line in a QQ plot confirming normal distributions for comparison. For time-course protein data, comparisons were performed by two-way ANOVA with Sidak's multiple comparisons test. P values <0.05 were considered statistically significant.

Results

RV Induction of CCL17 and CCL22 in Asthma Correlated with Markers of Disease

Time-course nasal expression of CCL17 and CCL22 from a human RV challenge study in subjects with mild to moderate asthma and healthy volunteers has previously been reported (20). In the current study, we reanalyzed these data by plotting baseline (Day 0) nasal CCL17 and CCL22 protein expression and peak expression during the infection to determine correlations with immunological and clinical outcomes, as previously described (5). At baseline, CCL17 protein was higher in nasosorption samples from subjects with asthma compared with healthy controls. Peak CCL17 was also higher in asthma during RV infection. For CCL22, baseline levels were nonsignificantly ($P = 0.072$) higher in asthma versus healthy and peak levels were significantly higher in subjects with asthma compared with healthy volunteers during RV infection (Figure 1A). Peak nasal CCL17 and CCL22 concentrations during infection were positively correlated with each other in both healthy subjects and subjects with asthma (Figure 1B). We previously reported that RV infection induced type-2 cytokines (IL-4, IL-5, and IL-13) and that IL-5 and IL-13 levels during infection in asthma positively correlated with respiratory symptom severity (5). In the current study, IL-4, IL-5, and IL-13 were positively correlated with peak nasal CCL17 (but not CCL22) production during RV infection (Figure 1C). Furthermore, CCL17 and CCL22 levels during RV infection correlated with peak upper respiratory symptom scores (Figure 1D), and at Day 4 after infection, bronchial CCL22 protein levels correlated with peak lower respiratory symptom scores in subjects with asthma (Figure 1E). These

data show that RV-induced CCL17 and CCL22 levels are differentially associated with clinical and immunological asthma exacerbation parameters and CCL17 (but not CCL22) positively correlated with type-2 cytokine expression.

RV Infection in Bronchial Epithelial Cells from Donors with Asthma Induces Higher Levels of CCL22 Compared with CCL17

Airway epithelial cells are a source of CCL17 and CCL22 (17, 34) and the primary site of RV infection (35). We next quantified CCL17 and CCL22 expression in RV-infected ALI-cultured BECs from donors with asthma (donor characteristics in Table 1). Infection with either major group RV-A43 or minor group RV-A1 did not significantly increase CCL17 mRNA expression (Figure 2A). However, RV infection did increase CCL22 mRNA expression. RV-A1 infection rapidly induced CCL22 expression, which peaked at Day 2 after infection, whereas induction by RV-A43 infection peaked at Day 4 (Figure 2B). We noted peak RV-induced CCL22 mRNA levels were ~10-fold higher than CCL17. CCL17 protein in apical supernatants were below the limit of detection, whereas CCL22 protein was detectable and significantly increased by RV-A1 infection (with a nonsignificant [$P = 0.088$] increase after RV-A43 infection) at Day 4 after infection (Figure 2C). Based on these time-course data, we selected baseline and Day 4 after infection as relevant time points to compare RV-induced CCL22 protein expression in ALI-cultured BECs from a separate cohort of donors with asthma and healthy control subjects without asthma ($n = 7$; donor characteristics in Table 2). To increase sample size, we combined the CCL22 protein data generated with the previous Day 4 CCL22 protein data from asthma BECs, providing $n = 14$ asthma donors infected with RV-A1 (Figure 2D). Infection of BECs from donors with asthma significantly increased CCL2 expression, which was higher ($P = 0.055$) than RV-induced CCL22 in BECs from healthy control donors (Figure 2D). We noted variability in RV-induced CCL22 levels between BEC cultures from donors with asthma but noted that variability did not correlate with atopic status determined by skin prick test positivity (Figure E2 in the data supplement). These data are consistent

with observed RV induction of CCL22 *in vivo* and indicate that airway epithelial cells from patients with asthma are primed to express higher levels of CCL22 compared with cells from healthy control subjects without asthma.

RV Infection Augments Type-2 Cytokine–induced STAT6 Activation

We next characterized transcriptional regulation of CCL17 and CCL22 during RV infection. Previous studies identified NF-κB and STAT6 binding sites in CCL17 and CCL22 promoters (14–16). Furthermore, STAT6 binding can have differential effects on target gene expression depending on the cellular context (19). Whether (and how) these transcription factors regulate expression of these chemokines in human airway epithelial cells during RV infection is unknown. We previously reported RV-induced epithelial cell NF-κB activation during RV infection (18). Here we investigated STAT6 activation following RV-A1 infection, in the presence of cytokine (IL-4/IL-13)–induced STAT6 phosphorylation in ALI-differentiated BEC cultures from healthy donors ($n = 6$). Type-2 cytokine treatment alone induced a near-significant ($P = 0.067$) increase in pSTAT6 levels, which was further increased with RV-A1 infection (Figure 3A).

To gain insight into potential mechanisms underlying increased STAT6 phosphorylation in ALI cultures following RV infection and stimulation with type-2 cytokines, we quantified expression of two Janus kinases (JAK1 and JAK2) that are activated by viral infection and have been shown to phosphorylate STAT6 (36, 37). IL-4/13 treatment significantly reduced constitutive expression of JAK1, whereas RV infection alone did not significantly deplete JAK1 expression (Figure 3A). RV infection reduced the suppressive effect of type-2 cytokines such that IL-4/13 treatment did not significantly reduce the expression of JAK1 compared with RV infection alone or compared with untreated cells (Figure 3A). For JAK2, RV infection increased expression above levels in type-2 cytokine–treated cells (Figure 3A). Again, RV infection partially reversed the suppressive effect of type-2 cytokine treatment such that the combination did not significantly reduce JAK2 compared with RV infection alone (Figure 3A). The data suggest that RV infection partially restores type-2 cytokine–suppressed JAK1
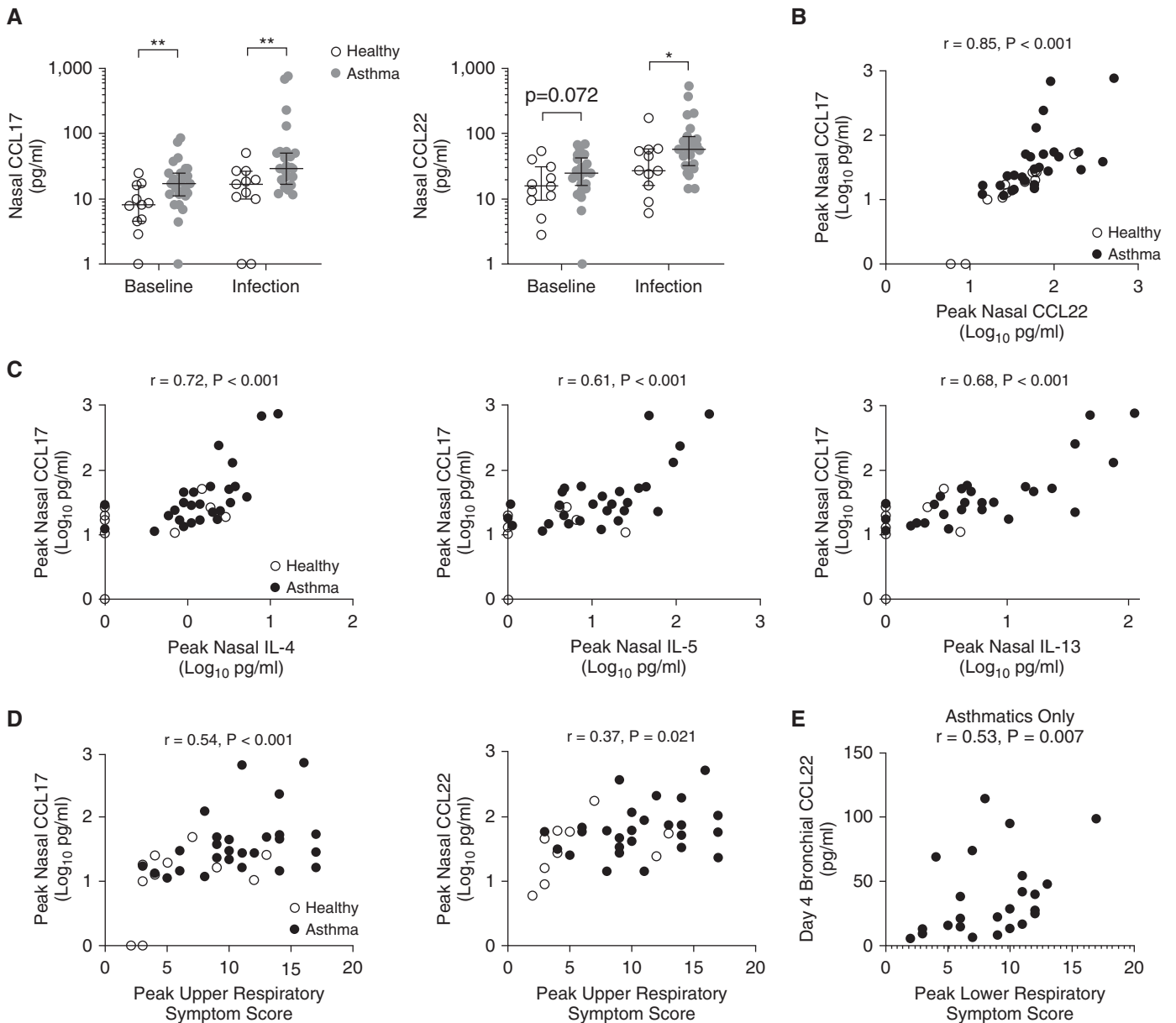
Figure 1. Increased *in vivo* RV-induced CCL17 and CCL22 in asthma is correlated with type-2 inflammation and disease severity. Individuals with asthma and healthy volunteers were infected with RV-A16 and nasal samples were obtained. (*A*) Protein levels of peak CCL17 and CCL22 in the nose. Median ± IQR. *$P < 0.05$ and **$P < 0.01$, healthy versus asthma at baseline or peak of infection analyzed by Mann-Whitney U test. (*B*) Correlation of peak nasal CCL17 and CCL22 levels. (*C*) Correlations of peak nasal CCL17 protein with peak nasal type-2 cytokine proteins (IL-4, IL-5, and IL-13). (*D*) Correlation of peak nasal CCL17 and CCL22 proteins with upper respiratory symptom scores. (*E*) Correlation of bronchial CCL22 protein with lower respiratory symptom scores. IQR = interquartile range; RV = rhinovirus.

expression, which could contribute to increased STAT6 phosphorylation observed following RV infection of type-2 cytokine–treated cells.

In addition to assessing expression of RV-induced kinases that phosphorylate STAT6, we also quantified negative regulators of STAT activation, namely, SOCS1 and SOCS3 (38). RV infection alone

as well in combination with type-2 cytokine treatment significantly increased SOCS1 and SOCS3 mRNA expression compared with untreated cells (Figure 3B). IL-4/IL-13 treatment with RV infection also increased SOCS3 expression compared with type-2 cytokine–treated BECs (Figure 3B). These data identified RV infection as the primary driver of SOCS3 expression. However, this

induction of SOCS3 was not sufficient to block RV-augmented type-2 cytokine–induced STAT6 phosphorylation, as shown in Figure 3A.

To determine if observed STAT6 phosphorylation led to increased transcriptional activity, we developed an *in vitro* assay system by treating BEAS-2B cells with IL-4 and/or infecting with RV.
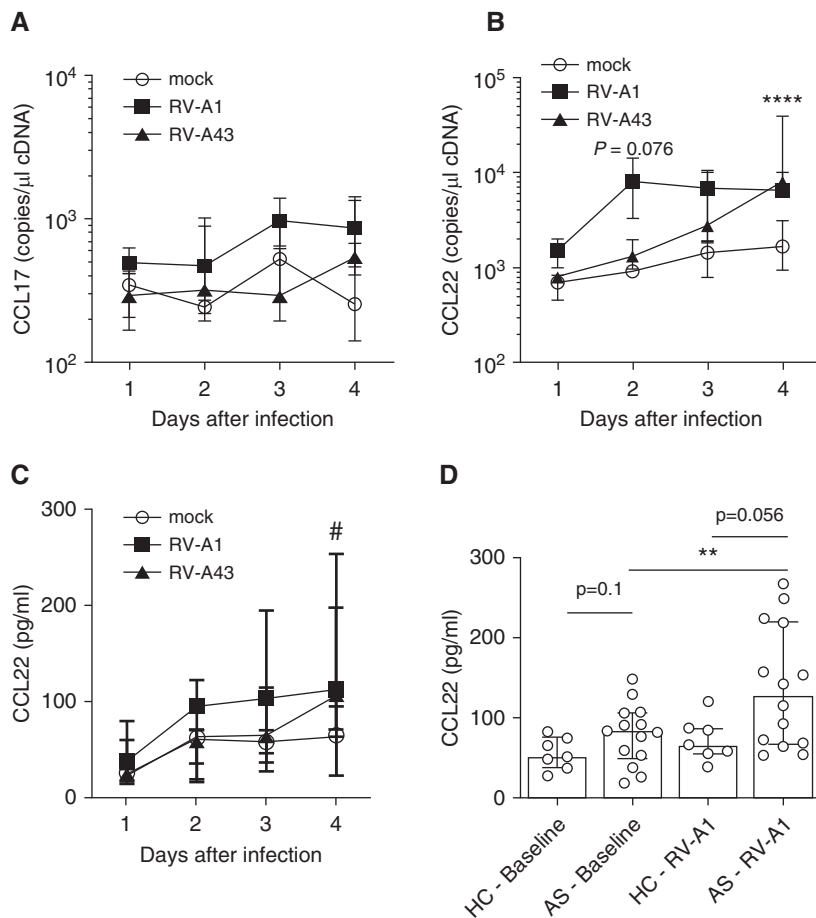
Figure 2. CCL22 induction by RV and increased expression by bronchial epithelial cells from donors with asthma. Air–liquid interface–differentiated bronchial epithelial cells from donors with asthma were infected with either RV-A1 or RV-A43. Time-course expression of (*A*) CCL17- and (*B*) CCL22-mRNA and (*C*) CCL22 protein. *n* = 6 donors for each time point. Median ± IQR was analyzed by two-way ANOVA with Dunnett's multiple comparison test. ****$P < 0.001$ RV-A43 versus mock and #$P < 0.05$ RV-A1 versus mock. (*D*) CCL22 protein expression at baseline and 4 days after RV-A1 infection in separate cohort of healthy control (HC) and asthmatic (AS) bronchial epithelial cells. *n* = 7 HC donors, *n* = 14 AS donors, median ± IQR analyzed by Mann-Whitney *U* test (HC vs. AS) or Wilcoxon matched pairs test (baseline vs. RV-A1). **$P < 0.01$.

Table 2. Clinical Characteristics of Healthy Donors and Donors with Asthma

	Healthy	Asthma
Number	8	8
Age, yr, mean (SD)	61.5 (13.6)	61.5 (8.8)
Sex, M/F	1/7	3/5
Atopy (SPT positive)	1/8	5/8**
Severity		
Moderate	N/A	1
Severe	N/A	7
FEV$_1$, % predicted (SD)	89.1 (12.4)	70.6 (21.5)*
FVC, % predicted (SD)	97.5 (15.9)	87.7 (12.6)
Daily ICS dose, beclomethasone equivalent, μg (SD)	N/A	287 (95.7)***

Definition of abbreviation: N/A = not applicable.
*Significantly different compared with healthy controls.
**$P < 0.01$ significantly different asthma vs. healthy (Mann-Whitney test).
***$P < 0.001$ significantly different asthma vs. healthy (Mann-Whitney test).

We initially confirmed expression of CCL17 and CCL22 protein by BEAS-2B cells. As in primary cells, RV infection alone did not induce detectable levels of CCL17 protein. However, combined IL-4 and RV treatment/infection significantly increased CCL17 protein (Figure E1A). RV infection alone increased CCL22 protein, whereas pretreatment with IL-4 reduced RV induction of CCL22 protein levels (Figure E1B).

Having established the utility of this BEAS-2B cell assay system to investigate the interaction between RV infection and type-2 cytokine treatment on CCL17 and CCL22 expression, we also used this system to examine STAT6 promoter activation following transfection of a STAT6-driven luciferase reporter plasmid. Compared with untreated cells, promoter activity was increased two- to threefold following RV infection (Figure 3C). IL-4 treatment significantly induced STAT6 promoter activation, compared with RV infection alone (approximately sevenfold), and combined IL-4 and RV exposure additively increased activation (>10-fold) (Figure 3C). These data provide evidence that RV infection alone is sufficient for low-level STAT6 activation in airway epithelial cells, and RV infection augments type-2 cytokine–induced STAT6 transcriptional activation.

STAT6 and NF-κB Activation Have Differential Effects on RV- and Type-2 Cytokine–induced CCL17 and CCL22 Expression

Experiments in BEAS2B cells indicated that type-2 cytokine/STAT6 differentially regulate CCL17 and CCL22. To further investigate transcriptional regulation of CCL17 and CCL22 expression, we assessed the effects of administering siRNAs targeting NF-κB (p65 or IKK-β) and STAT6 in A549 cells treated with IL-4 and/or infected with RV. We confirmed that siRNA administration reduced protein expression of the respective targets (Figure E3). As observed previously, the highest CCL17 levels were induced by a combination of IL-4 and RV-A1 exposure (Figure 4A). siRNAs targeting p65, IKK-β, or STAT6 all reduced IL-4/RV-A1–induced CCL17 production, compared with control siRNA treatment (Figure 4A). This was not the case for CCL22 expression, where the highest level of CCL22 expression was observed following RV-A1 infection alone

A

B

C
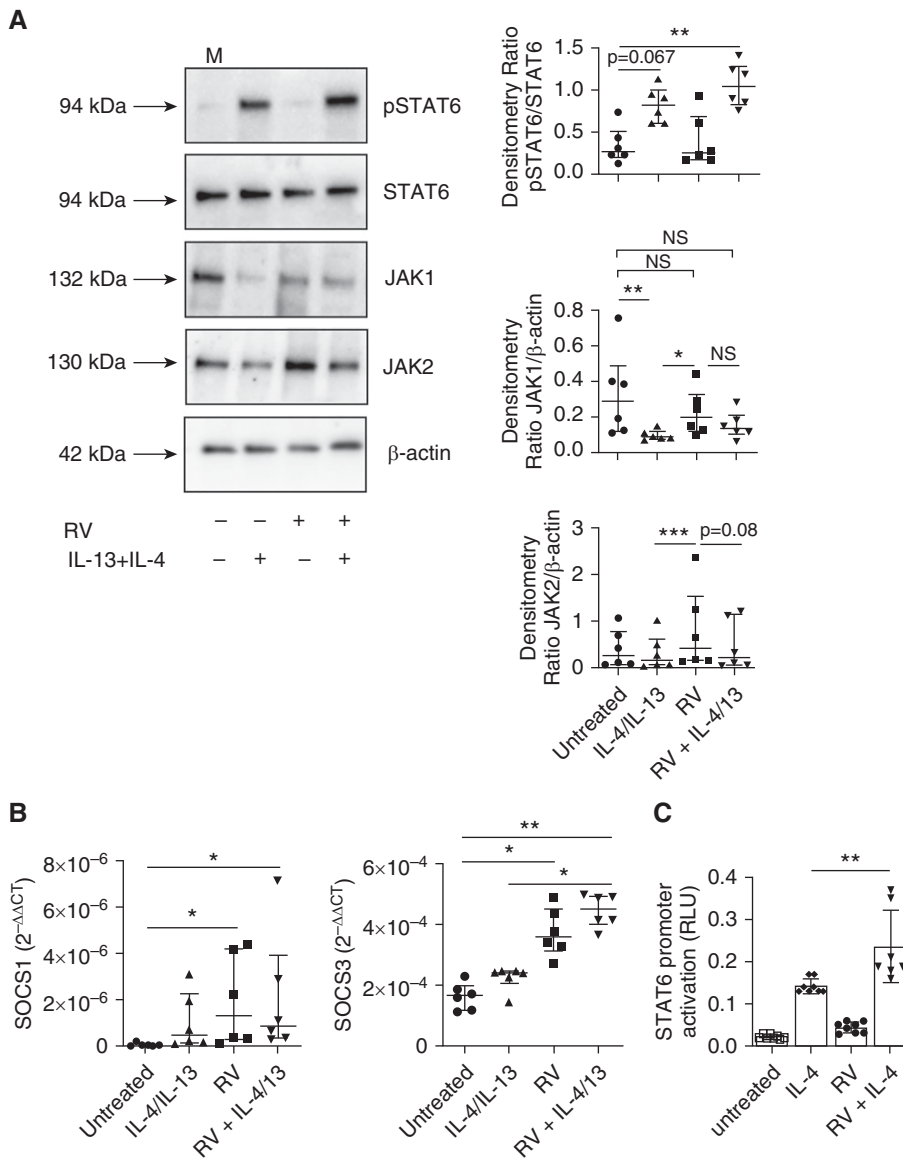
Figure 3. RV infection increased type-2 cytokine–induced STAT6 activation. Differentiated primary bronchial epithelial cells from $n = 6$ healthy donors were treated with type-2 cytokines or infected with RV. (*A*) Total STAT6, pSTAT6, total JAK1, JAK2, and β-actin protein expression was measured by immunoblot, representative blot, M molecular weight marker, and densitometry normalized to β-actin. (*B*) Fold change gene expression for SOCS1 and SOCS3 normalized to 18S RNA. Median ± IQR was analyzed by Friedman test with Dunn's multiple comparisons test. *$P < 0.05$, **$P < 0.01$, and ***$P < 0.001$ for indicated comparisons. (*C*) Luciferase activity RLU in BEAS-2B cells transfected with STAT6 reporter plasmid and infected with RV-A1 and or treated with IL-4, $n = 7$–8 replicate wells. Mean ± SD was analyzed by one-way ANOVA with Bonferroni multiple comparisons test. **$P < 0.01$. BEAS-2B = human bronchial epithelial cell line; JAK = Janus kinase; NS = nonsignificant; pSTAT6 = phosphorylated STAT6; RLU = relative light units; SOCS = suppressor of cytokine signaling; STAT6 = signal transducer and activator of transcription 6.

and significantly reduced by IL-4 treatment (Figure 4B). siRNA targeting p65 or IKK-β reduced CCL22 expression in RV-infected cells. In contrast, CCL22 expression increased following STAT6 knockdown in IL-4–treated cultures infected with RV

(Figure 4B). Inhibition of STAT6 expression also increased RV (alone)-induced CCL22 expression, providing further evidence of direct STAT6 activation by RV (Figure 4B). These data indicate that unlike CCL17, type-2 cytokine–induced

STAT6 activation negatively regulates CCL22 expression in RV-infected airway epithelial cells. We confirmed this observation in a more physiologically relevant system, observing that type-2 cytokine treatment (IL-4 and IL-13) suppressed RV-induced CCL22 protein expression in ALI-differentiated BEC cultures derived from healthy donors (Figure 4C).

Differential Kinetics of Expression of RV-induced CCL17 and CCL22 In Vivo

We also investigated pulmonary expression of CCL17 and CCL22 *in vivo* in a mouse model of RV infection (24) and observed s CCL17 and CCL22 protein expression in airway epithelium (Figure 5A). RV infection induced strong CCL17 staining exclusively in the bronchial epithelium (Figure 5A), with negligible staining in lung tissue from mock-infected or UV-inactivated RV inoculated mice. Constitutive CCL22 expression was apparent in lung tissue following mock infection or inoculation with UV-inactivated RV-A1. CCL22 was more broadly expressed in the lung than CCL17, with expression also detected in endothelial cells (Figure E4). CCL17 and CCL22 were also significantly elevated in BAL samples during RV-A1 infection, with CCL17 levels peaking at 1 day after infection and CCL22 peaking 2 days after infection, with both chemokines significantly elevated through 4 days after infection (Figure 5B).

RV-induced CCL17 and CCL22 Expression Are Differentially Regulated by STAT6 In Vivo

We next determined when STAT6 phosphorylation occurred in the lung during RV infection. We previously reported that RV infection induced NF-κB activation (18), so in the current study, we focused on STAT6. Increased levels of cytoplasmic pSTAT6 in lung tissue were observed 8 hours after RV-A1 infection (Figure 6A). Increased STAT6–DNA binding was observed in the nuclear fraction of lung protein samples from RV-infected mice (Figure 6B). This finding was confirmed in samples from four additional mice at 8 hours after infection, and binding specificity was confirmed using excess (100×) unlabeled probe (Figure 6B).

To determine the functional role of STAT6 activation on CCL17 and CCL22
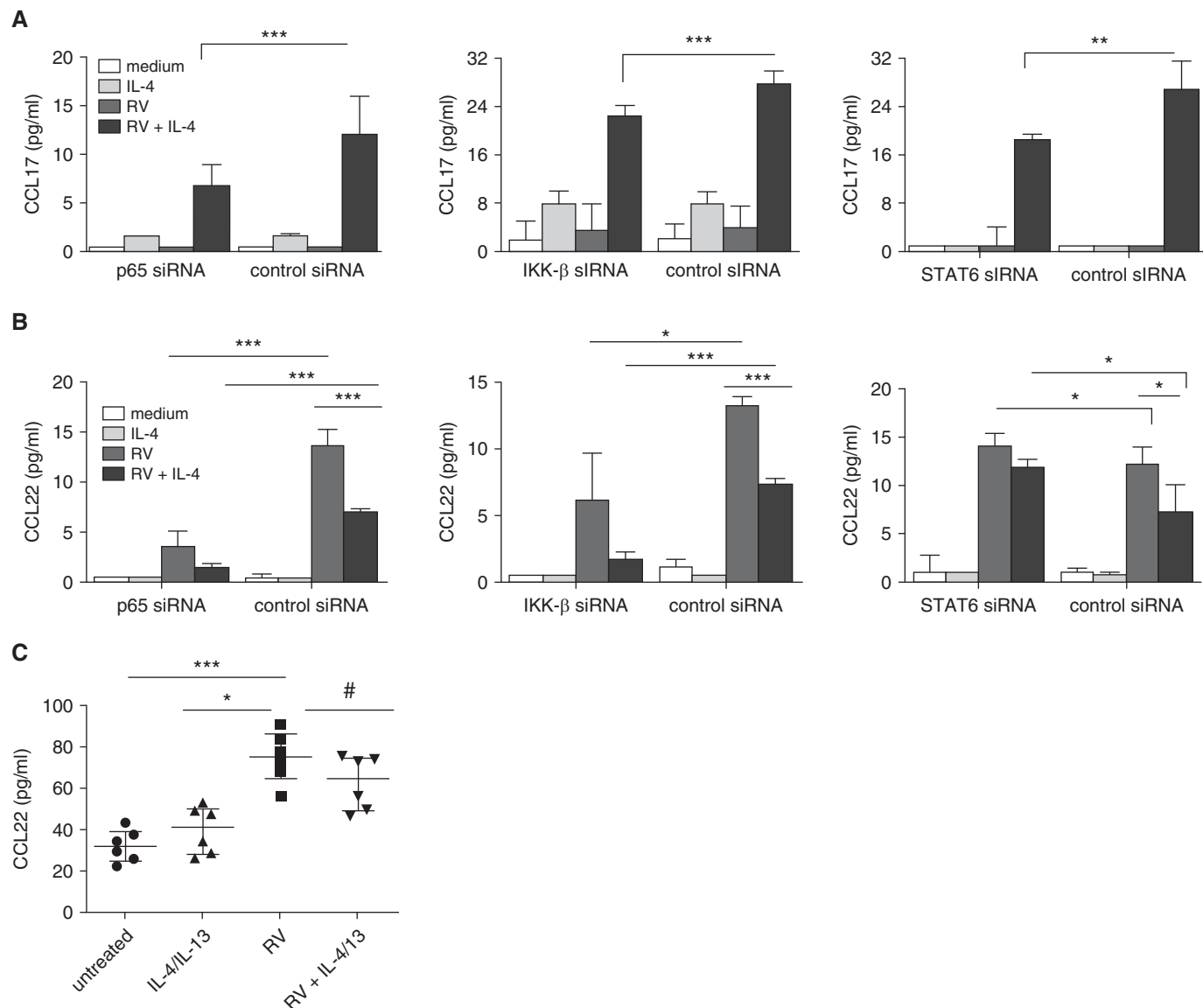
Figure 4. Differential STAT6 and NF-κB regulation of type-2 cytokine– and RV-induced CCL17 and CCL22 expression. A549 cells were transfected with NF-κB p65, IKK2, or STAT6-targeting siRNA or scrambled nontargeting control siRNA. Untreated cells (medium) or cells treated with IL-4 and/or RV-A1 were assessed for (*A*) CCL17- and (*B*) CCL22-protein expression. Data representative of at least three replicate wells. Median ± IQR analyzed by Mann-Whitney *U* test. *$P < 0.05$, **$P < 0.01$, and ***$P < 0.001$. (*C*) CCL22 protein expression by differentiated primary bronchial epithelial cells from $n = 6$ healthy donors untreated or treated with IL-4/IL-13 and/or infected with RV-A1, 96 hours after infection. Median ± IQR were analyzed by a Friedman test with Dunn's multiple comparisons. *$P < 0.05$, ***$P < 0.001$, and Wilcoxon matched-pairs test [#]$P < 0.05$.

production, we used an RV-A1 time course to identify chemokine expression 1-day after infection for assessment in STAT6ko mice. At 1 day after infection, lower levels of CCL17 were detected in BAL samples from STAT6ko mice compared with WT controls (Figure 6C). In contrast, but in agreement with our *in vitro* human data, STAT6 deficiency had no effect on CCL22 levels, indicating that STAT6 is not required to drive CCL22 expression in the

context of RV infection (Figure 6C). We also examined the role of NF-κB *in vivo*, using pharmacological IKK-β inhibition (Figure 6D) and genetically deficient p65^{+/−} mice (Figure 6E). Administration of the IKK-β inhibitor (PS1145) significantly reduced both CCL17 and CCL22 BAL protein levels following RV-A1 infection, compared with vehicle-treated controls (Figure 6D). Similarly, p65^{+/−} mice had reduced CCL17 BAL

protein levels after RV-A1 infection, compared with homozygous WT p65^{+/+} mice, following RV infection (Figure 6E). In p65^{+/−} mice, a trend ($P = 0.08$) toward reduced levels of CCL22 was also observed (Figure 6E). These data confirm that unlike CCL17, STAT6 is not required for RV-induced CCL22 expression. In contrast, NF-κB was required for expression of both chemokines following infection.

A

B
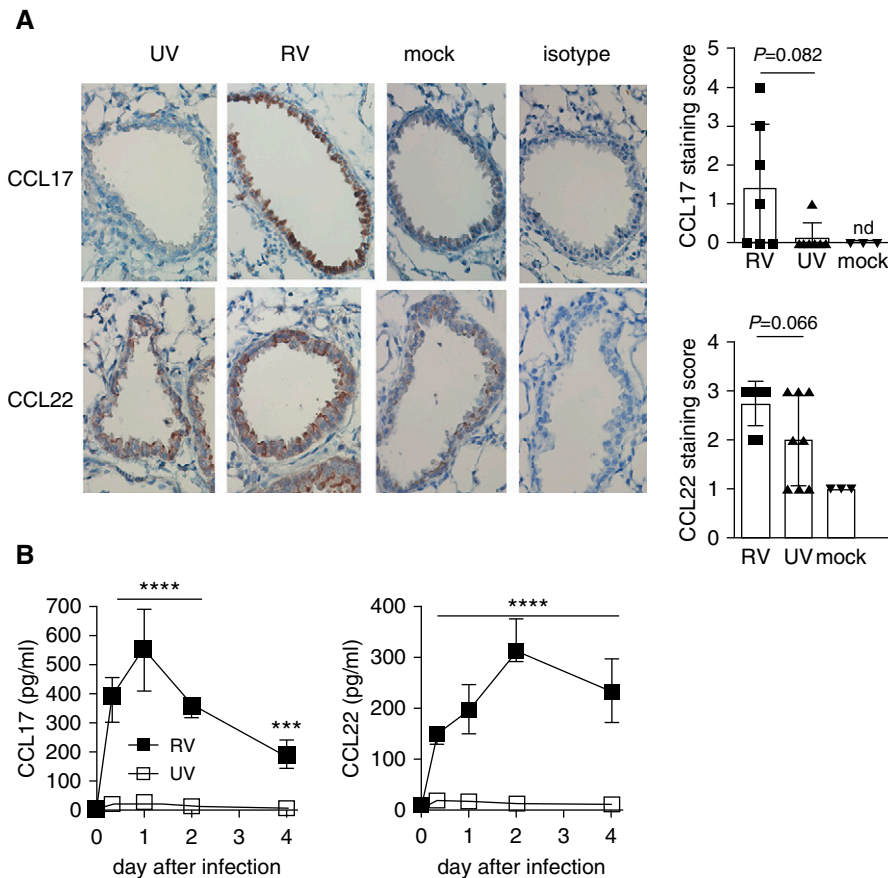
Figure 5. RV infection induces airway expression of CCL17 and CCL22. Mice were infected intranasally with RV-A1 (RV) or UV-inactivated RV-A1 (UV). Mock-infected mice were dosed intranasally with PBS. (*A*) Expression of CCL17 and CCL22 in the bronchi at 2 days after infection with immunohistochemistry staining score. Specificity of staining was confirmed with nontargeting isotype control antibody. $n = 7$–8 mice per group (for RV- and UV-treated mice). Mean ± SD, P values were calculated using Welch's t test. (*B*) Time course of CCL17 and CCL22 protein in BAL. $n = 4$ mice per group, representative of two independent experiments. Median ± IQR was analyzed by two-way ANOVA with Sidak's multiple comparison test. ***$P < 0.001$ and ****$P < 0.0001$. nd = not detectable.

STAT6 Expression Inhibits Viral Clearance and Expression of NF-κB–regulated Chemokines

To determine whether perturbation of STAT6 altered the RV-induced lung inflammatory milieu, we performed an RV-infection time-course analysis in WT and STAT6ko mice. At 8 hours after infection, viral load was not different between WT and STAT6ko mice. In contrast, by 24 hours after infection, lung viral load was ~10-fold lower in STAT6ko mice compared with WT controls (Figure 7A). RV infection induces airway neutrophilic inflammation, and we noted a consistent trend for increased neutrophils in BAL samples isolated from STAT6ko mice (Figure 7B). Furthermore, this was associated with significantly increased expression of the NF-κB–regulated

neutrophil-recruiting chemokines CXCL1 and CXCL2 in BAL fluid from STAT6ko mice. In contrast, IFN-λ levels were not increased in STAT6ko mice compared with WT mice (Figure 7C).

Discussion

This study interrogated the regulation of RV-induced CCL17 and CCL22 as a framework to better understand the interplay between two key inflammatory pathways (i.e., STAT6 and NF-κB), which collectively underpin the pathogenesis of asthma exacerbations. To do this, we used a human RV experimental infection model and *in vitro* airway epithelial cell and mouse RV infection models to show that

blocking STAT6 activation alone (particularly in the context of viral infection and NF-κB activation) will not completely inhibit inflammatory cell trafficking via chemokines such as CCL22 (where STAT6 activation may restrict expression).

We have previously reported time course of CCL17 and CCL22 protein expression in nasal and bronchial secretions in a human RV experimental infection model, in healthy volunteers and subjects with asthma (20). We reanalyzed these data to identify the peak expression level for each subject so that it could be correlated to type-2 cytokine production. This approach has been used previously to define clinical and immunological correlates of expression of other mucosal–epithelial–expressed inflammatory cytokines such as IL-33 (5). Peak expression of CCL17 (and not CCL22) correlated with IL-4, IL-5, and IL-13 expression in the nasal mucosa. This indicated that type-2 inflammation in combination with viral infection increased CCL17 expression. This conclusion is supported by *in vitro* experiments in human airway epithelial cells. In A549 cells, the combination of IL-4 treatment and RV infection was required for detectable expression of CCL17 protein. In primary human BECs differentiated at ALI, adding multiple type-2 cytokines (IL-4 and IL-13) with RV infection did not induce detectable CCL17 protein expression, suggesting that signals in addition to direct epithelial cell STAT6 activation, potentially mediated by immune cells, are needed for maximal expression by mucosal tissues. Immune cell augmentation of CCL17 production has been documented in other systems. For example, CCL17-expressing dendritic cells have been identified in intestinal mucosa and drive inflammation in a mouse colitis model (39).

Limited research has assessed the expression and regulation of CCL17 and CCL22 during respiratory virus infection in the context of asthma exacerbations (40–42). In a mouse model of RV infection, Nagarkar and colleagues assessed the lung inflammatory transcriptome and reported CCL17 as one of the most highly induced genes (>14-fold). Furthermore, CCL22 gene expression was significantly increased (greater than threefold) (43). Here we extended these results to report increased chemokine protein expression following RV infection in both human and mouse RV infection models. Our human *in vitro* BEC data demonstrated that RV subtypes
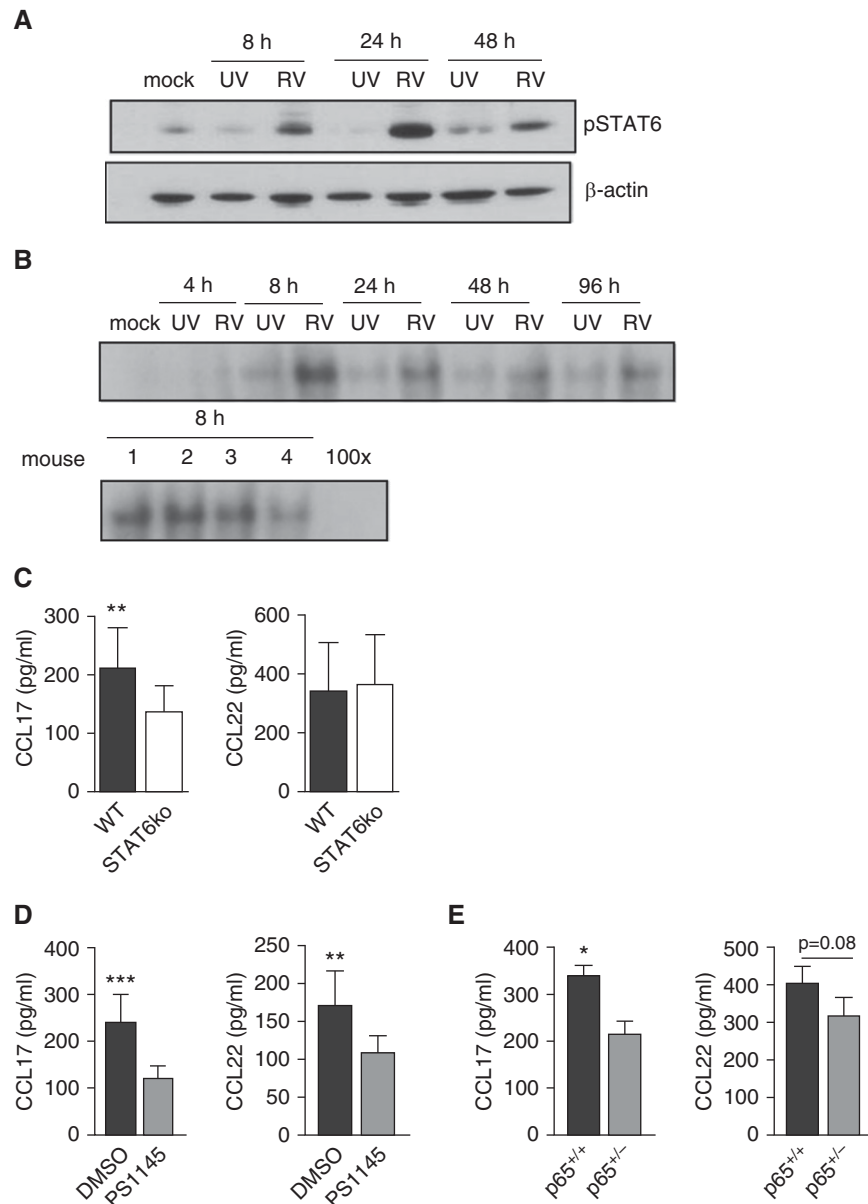
Figure 6. STAT6 and NF-κB differentially regulate RV-induced CCL17 and CCL22 expression *in vivo*. RV- or UV-treated mice. Mock–uninfected mice. (*A*) Representative Western blot time-course analysis of STAT6 phosphorylation in lung tissue cytoplasmic protein from *n* = 4 mice. (*B*) Time-course STAT6 DNA binding in lung tissue nuclear protein fraction measured by electrophoretic mobility shift assay. *N* = 4 mice shown for 8 hours after infection, 100× unlabeled probe. (*C*) Expression of CCL17 and CCL22 protein in BAL at 24 hours after infection of *n* = 5 WT and STAT6ko mice, pooled data from two independent experiments. Expression of CCL17 and CCL22 protein in BAL of RV infected mice (*D*) treated with vehicle (DMSO) or IKK2 inhibitor (PS1145), (*E*) in p65 homozygous positive (p65$^{+/+}$)- and p65 heterozygous (p65$^{+/-}$)-mice. *n* = 4 per group, pooled data from two independent experiments, mean ± SD. *$P < 0.05$, **$P < 0.01$, and ***$P < 0.001$, Mann-Whitney test. ko = knockout; WT = wild-type.

likely due to the higher RV infection doses and direct infection of the lower respiratory tract for the mouse infection model.

To look more broadly at RV infection and activation of NF-κB and STAT6 signaling pathways, we transfected siRNA into an epithelial cell line. Although both NF-κB- and STAT6 appear to be involved in regulating CCL17 production by alveolar epithelial cells, STAT6 negatively regulated CCL22 expression. This was further confirmed in STAT6$^{-/-}$ p65$^{+/-}$ mice and following IKK-β inhibitor PS1145 treatment, where CCL17 production was abrogated in the absence of NF-κB or STAT6, whereas CCL22 secretion was unaffected by altering STAT6. STAT6 has previously been reported to directly inhibit p65 translocation to the nucleus by inhibiting IKB-α phosphorylation in HeLa cells (44). Differential and direct interaction between NF-κB and STAT6 have previously been reported, with the two transcription factors synergistically enhancing luciferase expression by a synthetic inducible IL-4 reporter gene construct (45). Other studies have reported that IL-4–induced STAT6 activation reduced NF-κB DNA binding and IL-6 expression in certain cell types (46, 47). Ohmori and colleagues reported that STAT6 transactivating domain competed for the transcriptional coactivator CBP, and overexpression of CBP relieved the suppressive effect of STAT6 on TNF-α–induced NF-κB activation (26). Future studies will investigate STAT6 transactivation and interference with the activity of CBP coactivator on CCL17 versus CCL22 expression in the context of RV infection and type-2 cytokine stimulation in the lung.

STAT6 has been shown to either activate or repress type-2 cytokine–induced gene expression in different contexts. Georas and colleagues reported that IL-4 stimulation highly activated a synthetic multimerized STAT6-response element contained within the c/EBP-N4-luc reporter (19). However, IL-4–induced STAT6 activation negatively regulated native IL-4 promoter–driven IL-4 expression, leading the authors to conclude that the transcriptional function of STAT6 is dependent on promoter context (19). We previously reported that in a mouse model of RV-induced exacerbation, RV infection increased allergen (ovalbumin)-induced expression of both CCL17 and CCL22 (18). Increased type-2 cytokine expression is a feature of this model (24), so our data are consistent with STAT6 promoting both CCL17 and CCL22 expression. This further
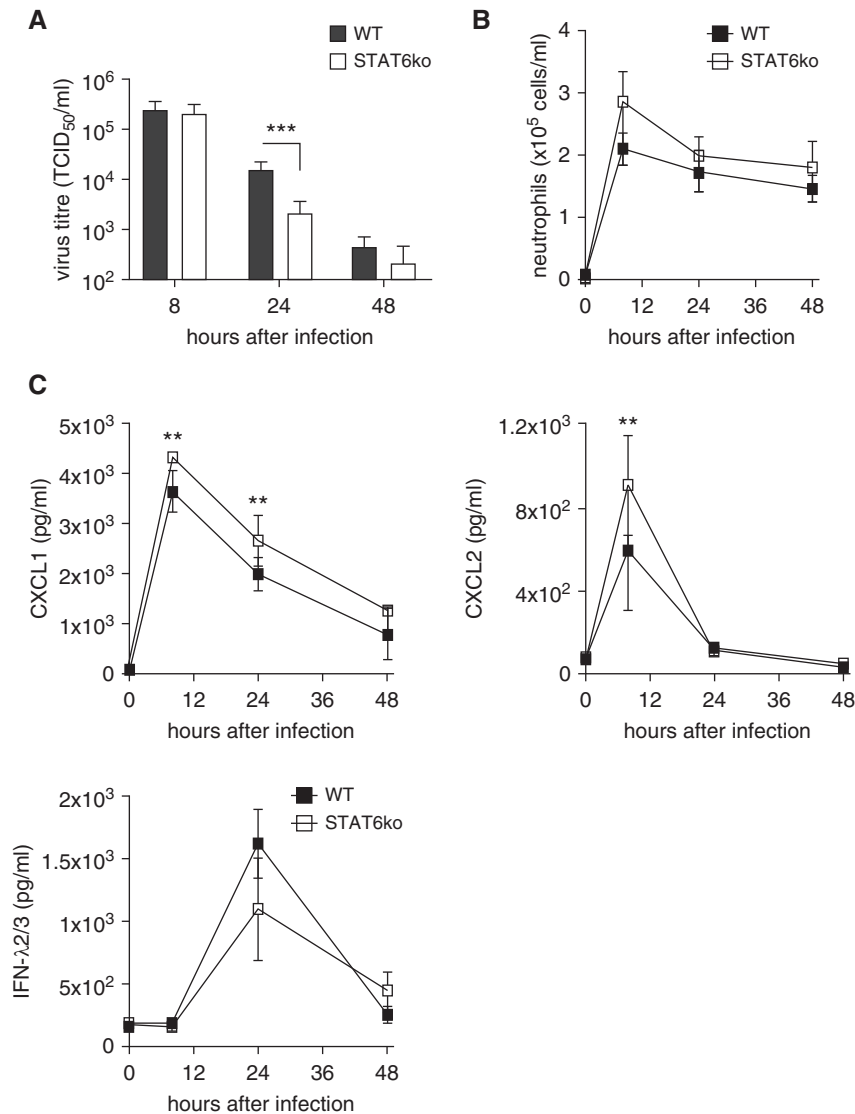
binding different receptors—major group (ICAM-1 receptor) and minor group (low-density lipoprotein receptor)—induced CCL22 expression, evidence that CCL22 expression is a general response to RV infection. Although we noted two- to threefold higher secretion of CCL22 and CCL17 within our *in vitro* and *in vivo* systems compared with the human experimental model, we attribute this as

Figure 7. STAT6ko mice have reduced lung viral load associated with increased expression of NF-κB–regulated chemokines. RV-infected WT or STAT6ko mice are shown. Time-course analysis of (*A*) titer of infectious virus in lung tissue, (*B*) neutrophils in BAL, and (*C*) CXCL1, CXCL2, and IFN-λ2/3 proteins in BAL at baseline (0 h) and 8, 24, and 48 hours after intranasal infection with RV-A1. $N = 5$ per group, representative of two independent experiments. Mean ± SD. **$P < 0.01$ and ***$P < 0.001$, two-way ANOVA with Sidak's multiple comparison test. $TCID_{50}$ = median tissue culture infectious dose.

In BEC cultures, CCL17 expression was synergistically increased by type-2 cytokines and RV infection, as has previously been noted following respiratory syncytial virus infection (41). However, the current study found that addition of IL-4 repressed RV-induced CCL22 and that siRNA-mediated knockdown of STAT6 relieved IL-4–induced suppression. Upon investigating upstream mediators of STAT6 signaling, we found that type-2 cytokines negatively regulated RV induction of both JAK1 and JAK2. A previous study in Schwann cells found that inhibition of JAK2/STAT pathways downregulated CCL22 gene expression (48), which complements the reduction in CCL22 secretion we observed when type-2 cytokines suppress JAK2 protein expression. Despite the upregulation in SOCS1 and SOCS3 gene expression that we observed following RV infection, RV infection still promoted JAK2 expression.

In summary, we identify differential transcriptional regulation and relationships with asthma disease parameters of RV-induced CCL17 and CCL22. Our data show that RV-challenged individuals with asthma had increased bronchial CCL22 associated with asthma symptoms, whereas peak CCL17 in the nose was associated with type-2 cytokine expression and upper respiratory tract symptoms. We demonstrated distinct STAT6-mediated transcriptional regulation of CCL17 and CCL22 during RV infection, while both chemokines were regulated by NF-κB. Thus, our findings provide new insight into the context-dependent expression of these often interchangeable CCR4 ligands. Our findings suggest that clinical trials targeting CCR4 (or downstream pathways) will be useful in asthma exacerbations, particularly those triggered by virus infection given the interplay of STAT6 and NF-κB in this clinical disease setting. In support of this, CCL17 and CCL22 were detectable in the nasal mucosa and RV-induced expression was higher in asthma compared with viral induction in healthy volunteers. Furthermore, bronchial CCL22 protein levels at Day 4 after experimental RV infection positively correlated with severity of lower respiratory tract symptoms in asthma. Further studies with selective inhibitors of CCR4/CCL17/CCL22 are needed to support therapeutically targeting this pathway in virus-induced asthma exacerbations. ■

highlights the context-dependent transcriptional activity of STAT6 in the interplay between type-2 allergic inflammation and RV infection. It is noteworthy that CCL17 (and not CCL22) protein expression significantly correlated with type-2 cytokine (IL-4, IL-5, and IL-13) expression in the nasal mucosa. This is consistent with type-2 cytokine–STAT6 activation preferentially driving CCL17 expression in the context of respiratory virus infection and acute exposure to type-2 cytokines. This raises the question of the net effect on CCR4-binding chemokine

expression if STAT6 selectively suppresses expression of CCL22, while promoting expression of CCL17. We also need to consider cell-specific expression profile, as BEC expression of CCL22 was higher than CCL17 and tissue expression *in vivo* (mouse lung) was also different. This highlights that the system is complex and that direct counterregulation by STAT6 may proportionally affect expression of CCL17 versus CCL22 such that the net effect on CCR4-mediated immune cell recruitment is zero depending on the specific circumstances.

References

1. Johnston SL, Pattemore PK, Sanderson G, Smith S, Campbell MJ, Josephs LK, et al. The relationship between upper respiratory infections and hospital admissions for asthma: a time-trend analysis. *Am J Respir Crit Care Med* 1996;154:654–660.
2. Fahy JV. Type 2 inflammation in asthma--present in most, absent in many. *Nat Rev Immunol* 2015;15:57–65.
3. Message SD, Laza-Stanca V, Mallia P, Parker HL, Zhu J, Kebadze T, et al. Rhinovirus-induced lower respiratory illness is increased in asthma and related to virus load and Th1/2 cytokine and IL-10 production. *Proc Natl Acad Sci USA* 2008;105:13562–13567.
4. Beale J, Jayaraman A, Jackson DJ, Macintyre JDR, Edwards MR, Walton RP, et al. Rhinovirus-induced IL-25 in asthma exacerbation drives type 2 immunity and allergic pulmonary inflammation. *Sci Transl Med* 2014;6:256ra134.
5. Jackson DJ, Makrinioti H, Rana BM, Shamji BW, Trujillo-Torralbo MB, Footitt J, et al. IL-33-dependent type 2 inflammation during rhinovirus-induced asthma exacerbations *in vivo. Am J Respir Crit Care Med* 2014;190:1373–1382.
6. Kawasaki S, Takizawa H, Yoneyama H, Nakayama T, Fujisawa R, Izumizaki M, et al. Intervention of thymus and activation-regulated chemokine attenuates the development of allergic airway inflammation and hyperresponsiveness in mice. *J Immunol* 2001;166:2055–2062.
7. Pilette C, Francis JN, Till SJ, Durham SR. CCR4 ligands are up-regulated in the airways of atopic asthmatics after segmental allergen challenge. *Eur Respir J* 2004;23:876–884.
8. Sekiya T, Yamada H, Yamaguchi M, Yamamoto K, Ishii A, Yoshie O, et al. Increased levels of a TH2-type CC chemokine thymus and activation-regulated chemokine (TARC) in serum and induced sputum of asthmatics. *Allergy* 2002;57:173–177.
9. Bonecchi R, Bianchi G, Bordignon PP, D'Ambrosio D, Lang R, Borsatti A, et al. Differential expression of chemokine receptors and chemotactic responsiveness of type 1 T helper cells (Th1s) and Th2s. *J Exp Med* 1998;187:129–134.
10. Weston CA, Rana BMJ, Cousins DJ. Differential expression of functional chemokine receptors on human blood and lung group 2 innate lymphoid cells. *J Allergy Clin Immunol* 2019;143:410–413, e9.
11. Lambrecht BN, Hammad H, Fahy JV. The cytokines of asthma. *Immunity* 2019;50:975–991.
12. Gonzalo JA, Pan Y, Lloyd CM, Jia GQ, Yu G, Dussault B, et al. Mouse monocyte-derived chemokine is involved in airway hyperreactivity and lung inflammation. *J Immunol* 1999;163:403–411.
13. Subramaniam JM, Whiteside G, McKeage K, Croxtall JC. Mogamulizumab: first global approval. *Drugs* 2012;72:1293–1298.
14. Nakayama T, Hieshima K, Nagakubo D, Sato E, Nakayama M, Kawa K, et al. Selective induction of Th2-attracting chemokines CCL17 and CCL22 in human B cells by latent membrane protein 1 of Epstein-Barr virus. *J Virol* 2004;78:1665–1674.
15. Liddiard K, Welch JS, Lozach J, Heinz S, Glass CK, Greaves DR. Interleukin-4 induction of the CC chemokine TARC (CCL17) in murine macrophages is mediated by multiple STAT6 sites in the TARC gene promoter. *BMC Mol Biol* 2006;7:45.
16. Wirnsberger G, Hebenstreit D, Posselt G, Horejs-Hoeck J, Duschl A. IL-4 induces expression of TARC/CCL17 via two STAT6 binding sites. *Eur J Immunol* 2006;36:1882–1891.
17. Sekiya T, Miyamasu M, Imanishi M, Yamada H, Nakajima T, Yamaguchi M, et al. Inducible expression of a Th2-type CC chemokine thymus- and activation-regulated chemokine by human bronchial epithelial cells. *J Immunol* 2000;165:2205–2213.
18. Bartlett NW, Slater L, Glanville N, Haas JJ, Caramori G, Casolari P, et al. Defining critical roles for NF-κB p65 and type I interferon in innate immunity to rhinovirus. *EMBO Mol Med* 2012;4:1244–1260.
19. Georas SN, Cumberland JE, Burke TF, Chen R, Schindler U, Casolaro V. Stat6 inhibits human interleukin-4 promoter activity in T cells. *Blood* 1998;92:4529–4538.
20. Hansel TT, Tunstall T, Trujillo-Torralbo MB, Shamji B, Del-Rosario A, Dhariwal J, et al. A comprehensive evaluation of nasal and bronchial cytokines and chemokines following experimental rhinovirus infection in allergic asthma: increased interferons (IFN-γ and IFN-λ) and type 2 inflammation (IL-5 and IL-13). *EBioMedicine* 2017;19:128–138.
21. Bardin PG, Sanderson G, Robinson BS, Holgate ST, Tyrrell DA. Experimental rhinovirus infection in volunteers. *Eur Respir J* 1996;9:2250–2255.
22. Alcamo E, Mizgerd JP, Horwitz BH, Bronson R, Beg AA, Scott M, et al. Targeted mutation of TNF receptor I rescues the RelA-deficient mouse and reveals a critical role for NF-κB in leukocyte recruitment. *J Immunol* 2001;167:1592–1600.
23. Quinton LJ, Jones MR, Simms BT, Kogan MS, Robson BE, Skerrett SJ, et al. Functions and regulation of NF-κB RelA during pneumococcal pneumonia. *J Immunol* 2007;178:1896–1903.
24. Bartlett NW, Walton RP, Edwards MR, Aniscenko J, Caramori G, Zhu J, et al. Mouse models of rhinovirus-induced disease and exacerbation of allergic airway inflammation. *Nat Med* 2008;14:199–204.
25. Bartlett NW, Singanayagam A, Johnston SL. Mouse models of rhinovirus infection and airways disease. *Methods Mol Biol* 2015;1221:181–188.
26. Ohmori Y, Hamilton TA. Interleukin-4/STAT6 represses STAT1 and NF-κ B-dependent transcription through distinct mechanisms. *J Biol Chem* 2000;275:38095–38103.
27. Birrell MA, Hardaker E, Wong S, McCluskie K, Catley M, De Alba J, et al. Iκ-B kinase-2 inhibitor blocks inflammation in human airway smooth muscle and a rat model of asthma. *Am J Respir Crit Care Med* 2005;172:962–971.
28. Varani K, Caramori G, Vincenzi F, Adcock I, Casolari P, Leung E, et al. Alteration of adenosine receptors in patients with chronic obstructive pulmonary disease. *Am J Respir Crit Care Med* 2006;173:398–406.
29. Jayaraman A, Jackson DJ, Message SD, Pearson RM, Aniscenko J, Caramori G, et al. IL-15 complexes induce NK- and T-cell responses independent of type I IFN signaling during rhinovirus infection. *Mucosal Immunol* 2014;7:1151–1164.
30. Slater L, Bartlett NW, Haas JJ, Zhu J, Message SD, Walton RP, et al. Co-ordinated role of TLR3, RIG-I and MDA5 in the innate response to rhinovirus in bronchial epithelium. *PLoS Pathog* 2010;6:e1001178.
31. Mikita T, Campbell D, Wu P, Williamson K, Schindler U. Requirements for interleukin-4-induced gene expression and functional characterization of Stat6. *Mol Cell Biol* 1996;16:5811–5820.
32. Hackett TL, Shaheen F, Johnson A, Wadsworth S, Pechkovsky DV, Jacoby DB, et al. Characterization of side population cells from human airway epithelium. *Stem Cells* 2008;26:2576–2585.
33. Singanayagam A, Glanville N, Girkin JL, Ching YM, Marcellini A, Porter JD, et al. Corticosteroid suppression of antiviral immunity increases bacterial loads and mucus production in COPD exacerbations. *Nat Commun* 2018;9:2229.
34. Panina-Bordignon P, Papi A, Mariani M, Di Lucia P, Casoni G, Bellettato C, et al. The C-C chemokine receptors CCR4 and CCR8 identify airway T cells of allergen-challenged atopic asthmatics. *J Clin Invest* 2001;107:1357–1364.
35. Reid AT, Sutanto EN, Chander-Veerati P, Looi K, Fung Li N, Iosifidis T, et al. Ground zero: the airway epithelium. In: Bartlett NW, Wark PAB, Knight D, editors. Rhinovirus infections: rethinking impact on human health and disease, 1st ed. London: Academic Press; 2019. pp. 314.
36. Cho W, Jeoung DI, Kim YM, Choe J. STAT6 and JAK1 are essential for IL-4-mediated suppression of prostaglandin production in human follicular dendritic cells: opposing roles of phosphorylated and unphosphorylated STAT6. *Int Immunopharmacol* 2012;12:635–642.
37. Palmer-Crocker RL, Hughes CC, Pober JS. IL-4 and IL-13 activate the JAK2 tyrosine kinase and Stat6 in cultured human vascular endothelial cells through a common pathway that does not involve the γc chain. *J Clin Invest* 1996;98:604–609.
38. Gielen V, Sykes A, Zhu J, Chan B, Macintyre J, Regamey N, et al. Increased nuclear suppressor of cytokine signaling 1 in asthmatic bronchial epithelium suppresses rhinovirus induction of innate interferons. *J Allergy Clin Immunol* 2015;136:177–188, e11.
39. Heiseke AF, Faul AC, Lehr HA, Förster I, Schmid RM, Krug AB, et al. CCL17 promotes intestinal inflammation in mice and counteracts regulatory T cell-mediated protection from colitis. *Gastroenterology* 2012;142:335–345.

40. Johnston SL, Pattemore PK, Sanderson G, Smith S, Lampe F, Josephs L, *et al*. Community study of role of viral infections in exacerbations of asthma in 9-11 year old children. *BMJ* 1995;310: 1225–1229.

41. Monick MM, Powers LS, Hassan I, Groskreutz D, Yarovinsky TO, Barrett CW, *et al*. Respiratory syncytial virus synergizes with Th2 cytokines to induce optimal levels of TARC/CCL17. *J Immunol* 2007; 179:1648–1658.

42. Zhang Y, Luxon BA, Casola A, Garofalo RP, Jamaluddin M, Brasier AR. Expression of respiratory syncytial virus-induced chemokine gene networks in lower airway epithelial cells revealed by cDNA microarrays. *J Virol* 2001;75:9044–9058.

43. Nagarkar DR, Wang Q, Shim J, Zhao Y, Tsai WC, Lukacs NW, *et al*. CXCR2 is required for neutrophilic airway inflammation and hyperresponsiveness in a mouse model of human rhinovirus infection. *J Immunol* 2009;183:6698–6707.

44. Nelson G, Wilde GJ, Spiller DG, Kennedy SM, Ray DW, Sullivan E, *et al*. NF-κB signalling is inhibited by glucocorticoid receptor and STAT6 via distinct mechanisms. *J Cell Sci* 2003;116:2495–2503.

45. Shen CH, Stavnezer J. Interaction of stat6 and NF-κB: direct association and synergistic activation of interleukin-4-induced transcription. *Mol Cell Biol* 1998;18:3395–3404.

46. Donnelly RP, Crofford LJ, Freeman SL, Buras J, Remmers E, Wilder RL, *et al*. Tissue-specific regulation of IL-6 production by IL-4: differential effects of IL-4 on nuclear factor-κB activity in monocytes and fibroblasts. *J Immunol* 1993;151:5603–5612.

47. Takeshita S, Gage JR, Kishimoto T, Vredevoe DL, Martínez-Maza O. Differential regulation of IL-6 gene transcription and expression by IL-4 and IL-10 in human monocytic cell lines. *J Immunol* 1996;156:2591–2598.

48. Fletcher JS, Springer MG, Choi K, Jousma E, Rizvi TA, Dombi E, *et al*. STAT3 inhibition reduces macrophage number and tumor growth in neurofibroma. *Oncogene* 2019;38:2876–2884.